Journal of Electronic Materials, Vol. 25, No. 8, 1996

Reduction of CdZnTe Substrate Defects and Relation to Epitaxial HgCdTe Quality

S. SEN, C.S. LIANG, D.R. RHIGER, and J.E. STANNARD

Santa Barbara Research Center, Goleta, CA 93117

H.F. ARLINGHAUS

Atom Sciences, Inc., Oak Ridge, TN 37830

We have conducted annealing experiments on CdZnTe wafers to restore stoichiometry, eliminate or reduce second-phase (Cd or Te) inclusions, and investigate effects on the quality of epitaxial HgCdTe grown on the thermally treated substrates. Two categories of second phase features were revealed in these materials. Category 1 has a star-like shape with sixfold symmetry (as seen by infrared transmission microscopy) and a central core consisting of cadmium. These stars were observed only in the more stoichiometric materials (having good infrared transmission characteristics). Category 2 consists of triangular, hexagonal, and irregular shaped tellurium inclusions which are present in the off-stoichiometry materials (which exhibit strong IR absorption). Substrates were annealed at temperatures ranging from 500 to 700°C for one to seven days, in vapor derived from elemental Cd or $Cd_{1-x}Zn_x$ alloy (x = 0.005). These anneals were able to eliminate the excess IR absorption and decrease the apparent sizes of both categories of second-phase features. It was found that pinhole-like morphological defects on the surface of a HgCdTe layer grown by liquid phase epitaxy can be caused by Cd and Te inclusions located within the CdZnTe substrate near the interface. Additionally, measurement and spatial mapping of copper concentration by sputter initiated resonance ionization spectroscopy showed 10 to 100 times higher Cu concentration in the inclusions than in the surrounding matrix areas.

Key words: Annealing, CdZnTe, defects, HgCdTe, impurities, inclusion, IR absorption, liquid phase epitaxy, second-phase, sputter initiated resonance ionization spectroscopy (SIRIS), stoichiometry

INTRODUCTION

Defects in epitaxial HgCdTe material can cause outages of single or multiple pixels in an IR detector array, if they fall within or close to any junction.[1-4] The effects are more pronounced at temperatures low compared to 78K because other current sources, such as diffusion, rapidly diminish as the temperature is reduced, whereas the leakage due to defects does not fall rapidly. Thus, isolated material defects will cause an array to be much more nonuniform when tested at 30K, for example, than at 78K. Since some of the morphological defects in the HgCdTe epitaxial layer leading to diode failure have their origin in the underlying CdZnTe substrate, it is important to minimize the number of these defects in the substrate for improved detector performance at low temperature and low photon flux levels. The types of defects which occur in CdZnTe substrate material range from point, line, and planar defects to second-phase inclusions and precipitates.

CdZnTe crystals grown by the Bridgman process are known to have deviation from stoichiometry at the growth temperature and during the cool-down period, which manifests itself as excess point defects (vacancies), inclusions, or precipitates in the grown crystal. We have found that some CdZnTe substrates grown by the vertical Bridgman process[5] exhibit poor infra-

(Received October 4, 1995; revised April 12, 1996)

Table I. Two Types of CdZnTe Substrates and the Inclusion-Related Defects Found in Each

Type of CdZnTe (as grown)	Category	Features Visible in IR Transmission Microscopy (≥10 μm diameter)	Composition of Core of Feature
TRANSPARENT	1	star	Cd
(Good IR Transmission, 2.5–16 μm)	0	round	void
ABSORBING	2	triangular	Te
(Strong IR Absorption, 2.5–16 μm)	2	hexagonal	Te
	2	irregular	Te
	0	round	void

Note: The second column indicates the category number assigned in the text.

red (IR) transmission (below 60%) for wavelengths between 2.5 and 16 μm. This is attributable to the presence of a high density of metal vacancies.[5] In addition, second-phase inclusions or precipitates are a well known occurrence, some of which can lead to diode-killing defects in the HgCdTe epitaxial layers. Recent studies[6,7] discussed ways to minimize Te precipitates in CdZnTe substrates and the annealing behavior of these precipitates based on their size. It was also reported[7] that diode arrays on long wavelength infrared (LWIR) HgCdTe epitaxial layers (grown from Te-rich melt) show improved R_0A uniformity if the CdZnTe substrates have been annealed to minimize Te precipitates, as compared to those fabricated with unannealed substrates. Gettering of impurities by inclusions in CdZnTe and their subsequent release to epitaxial HgCdTe layers have been investigated recently.[8]

Gettering of copper by tellurium inclusions in CdZnTe substrates and the role of copper for inducing type conversion in n-type HgCdTe films were also reported recently.[9]

In this study, we

- report on the characterization and annealing behavior of both Cd and Te inclusions found in CdZnTe substrates,
- show surface defect characteristics of CdZnTe substrates as a result of annealing,
- show effects on the epitaxial HgCdTe layer properties grown on annealed substrates from Hg-rich melts,[10] and
- show recent results from measurements of copper concentrations in and around Cd and Te inclusions in CdZnTe by sputter initiated resonance ionization spectroscopy (SIRIS).[11–13]

EXPERIMENTAL PROCEDURE

Cadmium Vapor Anneal

Annealing experiments under Cd vapor were performed on (111) $Cd_{0.96}Zn_{0.04}Te$ substrates grown by the vertical Bridgman process.[5] In the present work, the substrates could be divided into two broad types, transparent and absorbing, as listed in Table I. Those called absorbing have a high density of as-grown metal vacancies, which are revealed by strong IR absorption[5] between 2.5 and 16 μm. The other type by contrast is called transparent because of its excellent IR transmission characteristics. Among the substrates available to us for examination, representing dozens of boules, the great majority belonged to the transparent type. Although no sample of CdZnTe is perfectly stoichiometric, the stoichiometry of the transparent type is better than that of the absorbing.

In this study, all the absorbing substrates were selected from one boule and the transparent substrates were selected from six different boules. They were chemomechanically polished on both faces using 1% Br_2 in 50/50 methanol/ethylene glycol on a soft polishing pad. Pairs of transparent and absorbing substrates were then annealed for one to seven days at temperatures ranging from 500 to 700°C under Cd vapor. At each annealing temperature the Cd source within the ampoule was maintained at a temperature 50°C below that of the substrate.

The following characterizations were performed on each substrate wafer before and after anneal: (a) mapping the near-surface inclusion densities, while counting the buried inclusions (125–250 μm deep) in a 1 cm^2 area, (b) photographing inclusions with a polarizing IR microscope at seven different locations, (c) measuring the IR transmission (2.5–16 μm), (d) obtaining the Cu $K_{\alpha 1}$ x-ray rocking curve (333) reflection full width at half maximum (FWHM) values for average crystalline quality, and (e) performing photoluminescence (PL) measurements for the surface Zn compositions.[14]

To determine the composition of the second-phase regions in the CdZnTe, they were exposed in cross section and analyzed by energy dispersive x-ray (EDX) technique. To maintain the composition of these inclusions, no chemical etchant was used in the polishing process. Instead, the polishing was done mechanically with alumina (Al_2O_3) grit in deionized (DI) water. For samples, one transparent wafer containing star-like inclusions and two absorbing CdZnTe wafers (one unannealed and the other having been annealed in Cd vapor at 670°C for three days) were selected. One micron size Al_2O_3 was used to remove 25 μm from the Te-face (B-face) of the wafers and 0.05 μm

Al_2O_3 was used to remove 15 μm from the Cd-face (A-face) in order to expose the inclusions.

Cd-Zn Alloy Vapor Anneal

Liquid phase epitaxy (LPE) $Hg_{1-x}Cd_xTe$ layers grown on the Cd annealed substrates revealed morphological defect features suggesting that additional defects may be present in the substrates as a result of the Cd anneals. Several experiments were carried out to investigate further these anneal-induced defects. Since these defects are produced in both the transparent and absorbing materials, only the transparent substrates were used in these studies to simplify the interpretation of the results.

Vydyanath[15] suggested that Zn is depleted from the substrate surface during the Cd anneal thus generating additional defects on and near the surface region, and that this surface decomposition can be prevented by using the $Cd_{1-x}Zn_x$ alloy (x = 0.005) as the source of the vapor during annealing instead of Cd alone.

To study the effects of Cd-Zn anneal on CdZnTe, transparent substrates were used from the same boule. Each substrate was scribed into three sections. All three sections were chemomechanically polished and the surface defects on the Cd face were mapped with an infrared polarizing microscope and the x-ray rocking curve FWHM was measured at three locations in each section.

The first section was reserved as a control for later epitaxial layer growth. The second section was annealed at 700°C for three days with an overpressure of Cd-Zn vapor supplied by a reservoir of $Cd_{1-x}Zn_x$ (x = 0.005) alloy. The third section was used for annealing with Cd only at the same temperature and time for comparison. As before, the Cd-Zn or Cd source was held 50°C below the wafer temperature. Changes in surface Zn concentration were carefully measured by photoluminescence, and the average surface defects (Cd face) were measured by x-ray rocking curve FWHM. HgCdTe LPE layers were then grown on all three sections. Properties of the HgCdTe layers were evaluated as described below.

Measurement of Copper in Cd and Te Inclusions by SIRIS

We reported in 1993[16] the use of SIRIS for sensitive and quantitative measurements of copper concentration in CdZnTe substrates and HgCdTe epitaxial layers. The technique is extremely sensitive and accurate for measuring impurities down to the parts per trillion range (low $10^{13}/cm^3$) and does not suffer from the usual drawbacks of the secondary ion mass spectroscopy (SIMS) technique, such as surface and matrix effects. SIRIS measurements were performed at Atom Sciences using the system described elsewhere.[11-13] For this measurement, CdZnTe samples were specially prepared by Al_2O_3 grit polishing for capture and identification of the chemical composition of the inclusions as described above. Scanning electron microscope (SEM) photographs were taken of the exposed inclusions and their composition (Cd or Te) was determined by EDX. Samples were taken

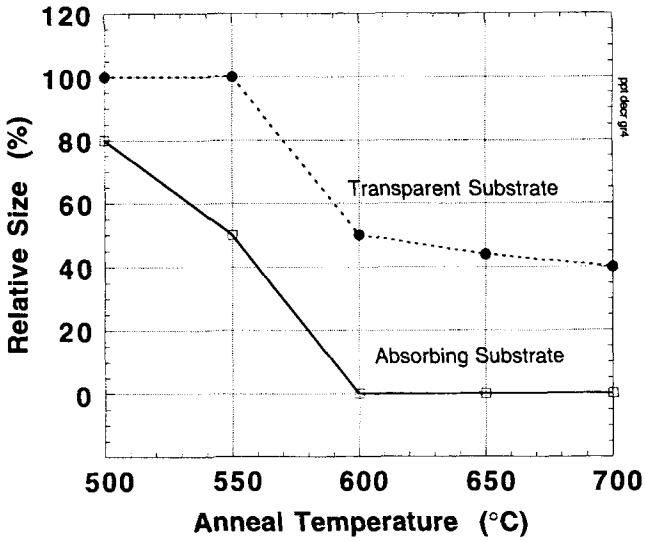

Fig. 1. Decrease in the apparent size of inclusions in CdZnTe substrates vs annealing temperature, for seven-day anneals in Cd vapor. Both transparent and absorbing substrates (as defined in Table I) were annealed.

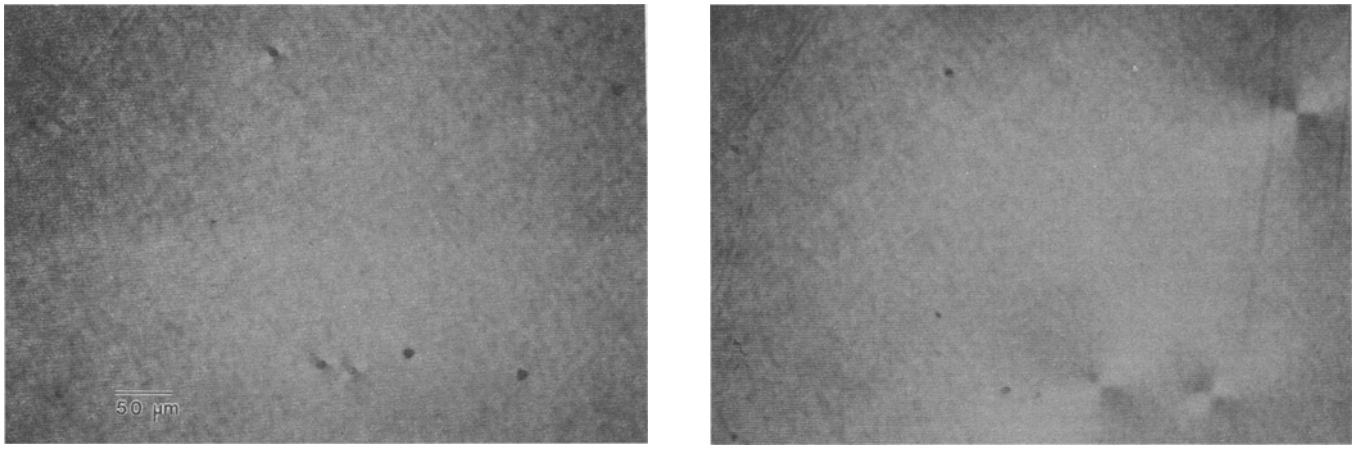

a b

Fig. 2. Polarized IR transmission images of the same area of an absorbing CdZnTe substrate: (a) before anneal, and (b) after annealing in Cd vapor at 600°C for seven days.

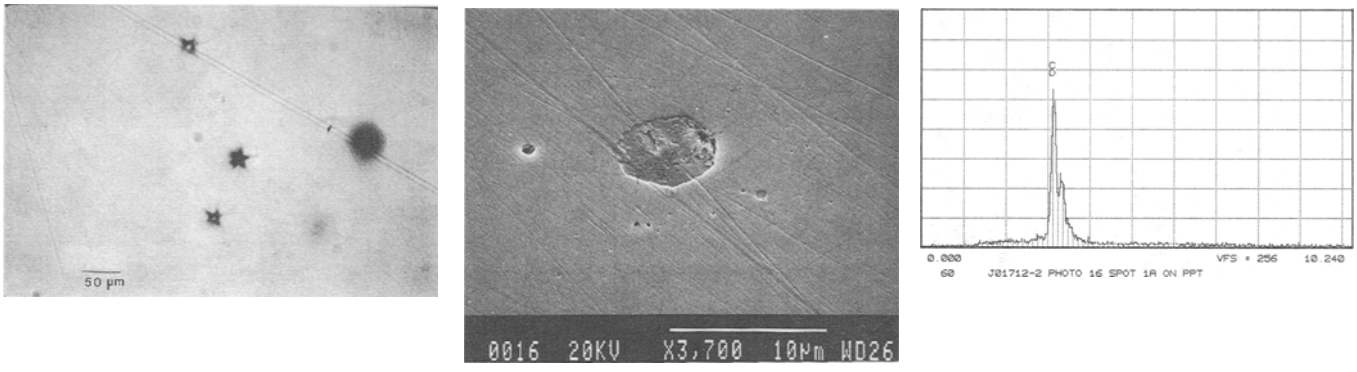

a b c

Fig. 3. Micrographs of the unannealed transparent CdZnTe substrate having a grit-polished surface: (a) IR transmission image showing three star-shaped defects. The round object to the right is a star-shaped defect that is out of focus, (b) high magnification SEM image of the inclusion that occurs at the center of a star, and (c) EDX spectrum of the inclusion in Fig. 3 (b). The composition is almost 100% Cd.

from two different boules. The sample containing Cd inclusions was obtained from a transparent boule and that with Te inclusions was obtained from an absorbing boule. In these samples, the typical size of the Cd inclusions was 12–15 μm, and that of Te inclusions was 15–30 μm. Spatial mapping of copper concentration in and around both Cd and Te second phases was performed with the sample temperature kept at 110K.

LPE $Hg_{1-x}Cd_xTe$ Layer (LWIR, x = 0.22) Quality

The effect of the substrate anneals on the subsequent Hg-melt LPE $Hg_{1-x}Cd_xTe$ (LWIR, x = 0.22) layer quality was evaluated by examination of the surface morphology of the layers using an optical microscope with Nomarski or polarized light contrast and comparison with pre-LPE images on the substrates at same locations, and by Hall effect measurements.

RESULTS

Cd Vapor Anneal

Examination of CdZnTe substrates from transparent and absorbing boules under infrared polarizing microscope has revealed two categories of readily observable defects. Category 1 has star-like features with sixfold symmetries plus a central core consisting of an inclusion and was found only in the transparent substrates. Category 2 consists of triangular, hexagonal, and irregular shaped inclusions found only in the absorbing materials. These two categories, plus the round features (called category 0), are listed in the third column of Table I. The typical size of the central core region of the star is 5–15 μm, whereas the dimensions of the category 2 inclusions ranged from 10 to 50 μm. Inclusions at the larger end of each range were less common. Cd vapor anneals were able to correct IR transmission in absorbing CdZnTe and decrease the apparent sizes of both categories of inclusions at various temperatures. The decreases in apparent size of inclusions (categories 1 and 2) vs annealing temperatures, for isochronal seven-day anneals in Cd vapor are shown in Fig. 1 for both transparent and absorbing CdZnTe substrates.

The size and shape of the star defects (category 1) in the transparent substrates remained unchanged after annealing for a period of seven days at 500 and 550°C (Fig. 1). However, the apparent size decreased progressively from 50 to 40% of the original size between annealing temperatures of 600 and 700°C. As the overall size of the defect started to shrink, the sixfold symmetry was no longer visible under polarized IR microscope. Also, when a near-surface defect of this kind is subjected to the Nakagawa etch,[17] a broad star pattern of etch pits is developed if the substrate has not been annealed, but the pattern is smaller and more compact on a substrate that has been annealed. A possible explanation can be given for these results. As shown below, the core of the star consists of a Cd inclusion. Thus, during the anneal, the imposed chemical potential of Cd would not promote dissolution of the inclusion itself, so that it would not shrink at all. However, the star represents a larger surrounding volume which is visible due to strain contrast in the IR image. A mechanical annealing of this strain may account for the observed shrinking of the defect feature.

In case of the absorbing substrates where the star shaped inclusions are not present, the category 2 inclusion size decreased by 20% after annealing at 500°C for seven days. At 550°C for 7 days, inclusions having an initial size below 40 μm either disappeared or reduced to a size less than 10 μm (resolution limit of the optical microscope), and inclusions initially greater than 40 μm reduced by 50%. At annealing temperatures of 600°C and higher, the size of these dropped below the detection limit and they may have been completely annihilated (Fig. 1). When examined under cross-polarized light in the IR microscope, resulting strain fields were observed surrounding the former sites of the inclusions, especially for those with initial size greater than 15 μm. Figure 2 shows polarized IR transmission images of an absorbing CdZnTe substrate: (a) before anneal and (b) after annealing in Cd vapor at 600°C for seven days. There are three distinctly triangular inclusions that shrank during the anneal to below detectable size, leaving behind bow-tie shaped strain fields. Some other features in

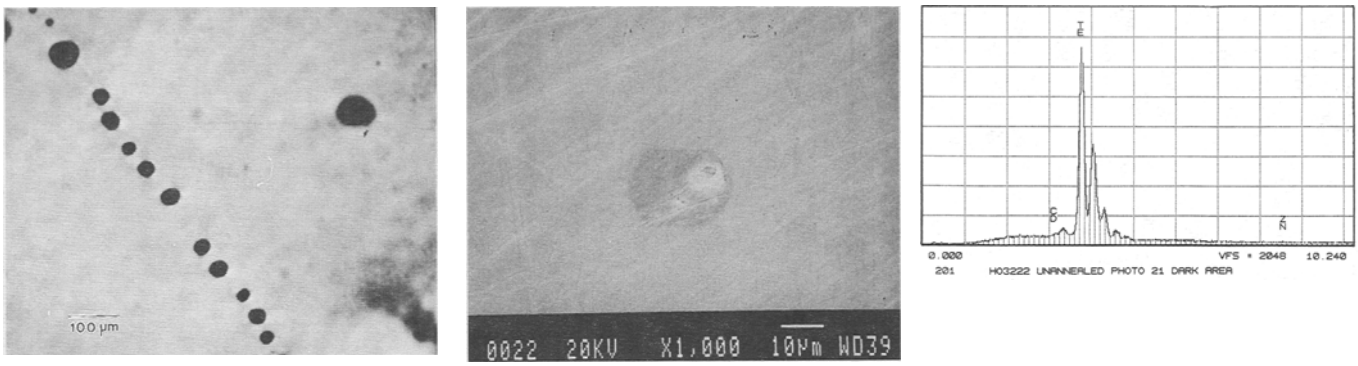

a b c

Fig. 4. Micrographs of the unannealed absorbing CdZnTe substrate having a grit polished surface: (a) IR transmission image showing hexagonal shaped inclusions. Some line up on a low angle grain boundary, (b) high magnification SEM image of the inclusion that lies toward the upper right of Fig. 4 (a). The inclusion is the dark hexagon, which is 24 µm left to right. (A hole appears within the upper right of the inclusion.) (c) EDX spectrum of the inclusion showing almost 100% Te.

the wafer are apparently unchanged. These are believed to be voids (category 0). In some substrates, a feature with a threefold symmetry was observed, which was later revealed by Nakagawa etch[17] to be dislocation clusters.

EDX data of the unannealed transparent substrate indicate that the inclusion in the center of the star-shaped defect is cadmium. This result is illustrated in Fig. 3, where part (a) shows the IR transmission image and part (b) shows a higher magnification SEM image, both on the grit-polished surface. The inclusion in Fig. 3b lies at the center of the star that appears near the middle of Fig. 3a. Scratches from the grit are also visible. Figure 3c is the EDX spectrum, showing almost 100% Cd, obtained within the inclusion in Fig. 3b. Cadmium enrichment was also found on the smaller features around the inclusions. Photographs taken from both the IR transmission microscope and the Nakagawa etched surface confirm that these inclusions can be identified with the stars defined as category 1 defects (Fig. 3). The formation of these star-like patterns is believed to occur shortly after growth when the boule is cooled from the growth temperature to room temperature. The stress due to thermal expansion differences and volume misfits between the Cd and CdZnTe results in punching out of dislocations in all <110> directions to relieve the stress.[18,19]

Observations of inclusions (category 2) representing the typical features found in the absorbing CdZnTe substrates before anneal are presented in Fig. 4. Figure 4a shows an IR transmission image of some hexagonal-shaped inclusions. The inclusion in Fig. 4b appears in cross section as a dark hexagon by SEM. Excess Te with very little Cd was found in this inclusion as shown in Fig. 4c. Holes of various sizes and shapes were also found inside some of the inclusions themselves. EDX data also indicate the presence of excess Te on the edges of the inclusion as well as the inside surface of the holes. Such holes may have been caused by fracturing of the Te during the grit polishing. The Cd anneal has been successful in converting second-phase Te into CdTe as suggested

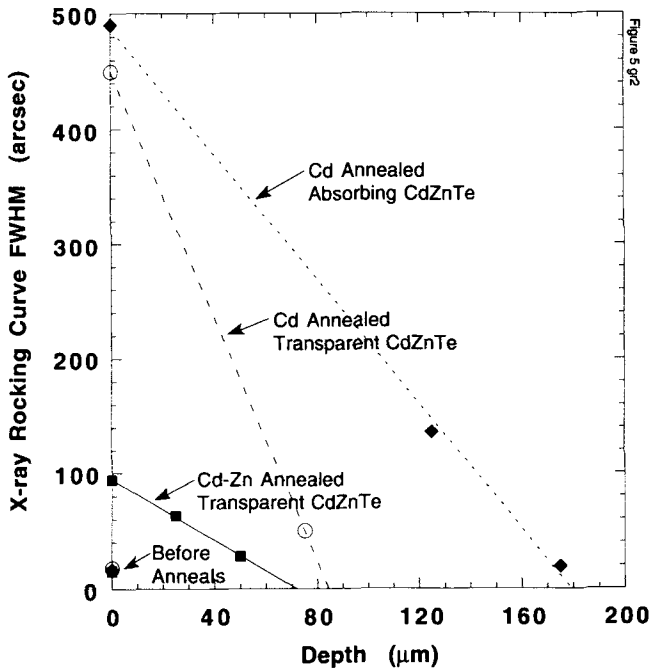

Fig. 5. Depth of damage profile of Cd-annealed absorbing substrate compared with Cd-Zn and Cd annealed transparent substrates. All were annealed at 700°C for three days.

by EDX data taken at the same sites after annealing.

Furthermore, observations indicate the presence of small voids (20–30 µm) that were previously thought to be precipitates when viewed under both the reflected light and infrared polarizing microscopes. These voids, which are defects of category 0 and are possibly created during growth,[20] could not be removed by a Cd anneal at any temperature. EDX detected CdZnTe both in the matrix near the void and on the inside edges of the void.

These annealing experiments also revealed that additional defects of a smaller size but greater number were generated on the substrate surface during the anneal. They were manifested as etch pits by the Nakagawa etch and as a broadening of the (333) x-ray rocking curve FWHM. The most likely cause is depletion of Zn from the substrate surface during the Cd

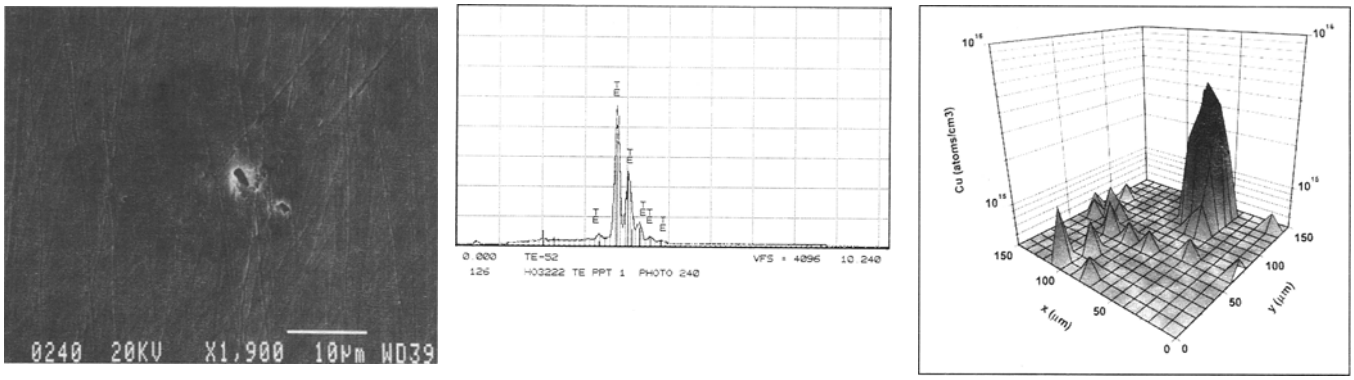

a b c

Fig. 6. SIRIS measurement of copper concentration in and around a Te inclusion in a CdZnTe substrate: (a) SEM photograph of Te inclusion, (b) EDX plot verifying composition of the inclusion, and (c) SIRIS map of Cu distribution in and around the inclusion measured by SIRIS imaging. The data show ten times higher copper concentration in the Te than in the matrix area.

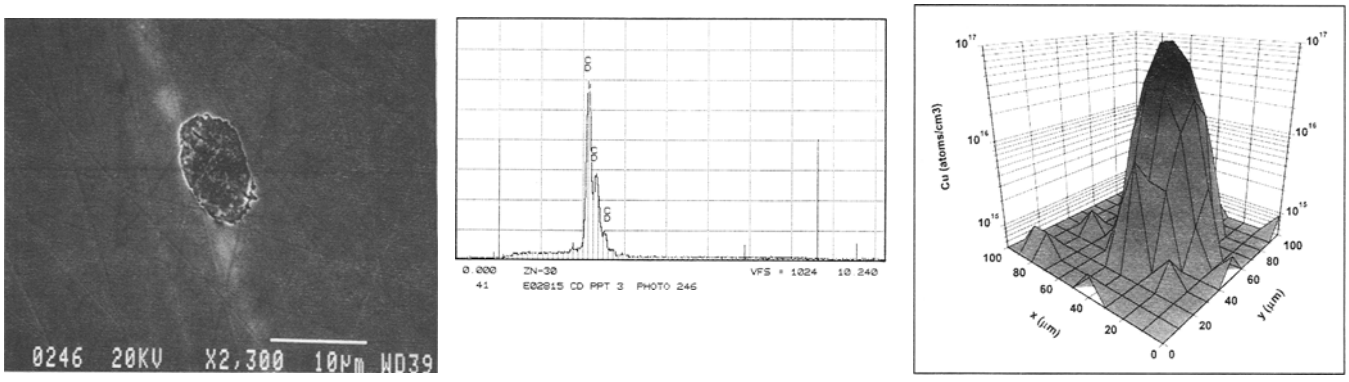

a b c

Fig. 7. SIRIS measurement of copper concentration in and around a Cd inclusion in a CdZnTe substrate: (a) SEM photograph of Cd inclusion, (b) EDX plot verifying composition of the inclusion, and (c) SIRIS map of Cu distribution in and around the inclusion measured by SIRIS imaging. The data shows 100 times higher copper concentration in the Cd than in the matrix area.

anneal. The depth of damage was found to range from 50 to 175 µm for annealing temperatures greater than 600°C. It was significantly deeper for absorbing substrates than for transparent CdZnTe, as described in the following section.

Cd-Zn Alloy Vapor Anneal

As discussed in the experimental section for the Cd-Zn alloy vapor anneal, additional annealing experiments were conducted to investigate the cause of the anneal-induced surface damage in CdZnTe substrates. Since these defects were present in both the transparent and absorbing materials, only the transparent substrates were used in these studies to simplify interpretation of the results. The samples were selected from the same boule. Annealing was performed at 700°C for three days, one substrate section with Cd-Zn alloy vapor and the other with Cd vapor for comparison. A third section was kept as an unannealed control sample.

The PL and the x-ray rocking curve FWHM measurements were taken at three different locations. The PL data show a 45% increase in the surface Zn concentration after the Cd-Zn anneal. By removing 25 µm from the surface however, the Zn content returned to pre-annealed value. The x-ray rocking curve FWHM data show an increase from 15 arcsec before the anneal to 94 arcsec after the anneal. By removing 50 µm from the annealed surface, the FWHM decreased to pre-annealed value. For the Cd annealed substrate, the Zn content decreased by 77% at the end of the 700°C/three-day Cd anneal. This finding agrees with Vydyanath's theory of the surface Zn loss during a Cd anneal.[15]

Also, the Zn concentration of the Cd annealed transparent substrate returned close to pre-annealed values after removing 25 µm from the annealed surface, and the damage depth was estimated to be slightly greater than 75 µm from x-ray FWHM values. However, in comparison, the damage depth on an absorbing substrate annealed at 700°C for three days under Cd overpressure was 175 µm, which is much greater than both the Cd-Zn and Cd annealed transparent substrates under the same conditions. Figure 5 compares the depth-of-damage profile for a Cd-annealed absorbing substrate with those of Cd-Zn and Cd annealed transparent substrates, all of which were annealed at 700°C for three days. As a measure of the effect of Zn loss, Fig. 5 shows that for transparent material the FWHM at the surface is 450 arcsec with the Cd anneal, whereas it is less than 100 arcsec for the Cd-Zn anneal.

Measurement of Copper in Cd and Te Inclusions by SIRIS

As discussed above, we identified two different compositions of second phase inclusions in CdZnTe, the star-shaped defect with a central core region containing excess Cd, and the triangular, hexagonal, and irregular shaped ones containing excess Te. To determine whether the inclusions of Cd and Te act as gettering centers for certain impurities like Cu, SIRIS was used to image and analyze copper concentrations inside the inclusion volume and within the matrix surrounding the inclusion. Samples from a transparent substrate for the star-like defect containing Cd at its core, and from an absorbing substrate for inclusions containing Te, were specially prepared by grit polishing. SEM images were taken of the features to be analyzed and their compositions were verified by EDX before performing the SIRIS analysis.

Figure 6 shows a Te inclusion in CdZnTe and the copper distribution measured by SIRIS: (a) SEM photograph of the inclusion, (b) EDX plot verifying the composition, and (c) SIRIS map of the Cu distribution in and around the inclusion. Figure 7 shows corresponding photographs and SIRIS data for a Cd inclusion. The size of the Te inclusion was 28 μm and the Cd inclusion was 12 μm. In case of the sample containing the Te second phase, SIRIS data shows a factor of ten higher copper concentration in the Te (mid-10^{15} cm^{-3}) than in the matrix area (mid-10^{14} cm^{-3}). For the sample with the Cd second phase, the copper concentration was up to 100 times higher in the Cd than in the matrix area. The spatial resolution of the mapping is limited by the ion beam diameter, which is about 40 μm. In the SIRIS map, for this reason, the peak appears to be broader than the inclusion itself, and the apparent maximum Cu concentration is likely to be four to eight times lower than the true value in the inclusion.

Thus, from SIRIS data it is clear that both Te and Cd inclusions getter Cu in CdZnTe. The greater difference between Cu concentration in the Cd inclusion and the matrix may imply a higher overall level of Cu in that sample compared with the sample containing the Te inclusion (the two samples being from different boules). Alternatively, the Cd may have a greater affinity for Cu.

LPE HgCdTe Layer Quality

Substrates annealed in Cd-Zn vapor and Cd vapor, as well as the controls (unannealed substrates from the same boule), were chemomechanically polished and the surface defects on the Cd-face were mapped with both the polarized reflected light and the infrared polarized microscopes. After LPE growth of $Hg_{0.78}Cd_{0.22}Te$ from a Hg-rich melt, examination of the layer morphology under the polarized reflected light microscope showed, for the layers on unannealed substrates, a correlation of pinhole-like defects with underlying near-surface inclusions in the substrate, but, for the layers on annealed substrates, additional irregular shaped defects were also found which had no obvious correlation with underlying substrate defects. Examples of the latter kind are shown in Fig. 8. The density of these additional defects in the HgCdTe was lower in layers grown on substrates annealed in Cd-Zn vapor than on those annealed in purely Cd vapor. Two possible explanations can be offered for this difference. The first relates to the procedure for monitoring the quality of the surface of the annealed substrate while it was being prepared for the LPE growth. For substrates that had received the Cd-Zn anneal, both the crystalline quality (measured by x-ray rocking curve) and the surface Zn concentration (measured by photoluminescence) were monitored and returned to the pre-annealed conditions by chemomechanically polishing down in steps of 25 μm. For substrates receiving the Cd anneal, however, only the etch pit density (EPD) was measured. Considering the greater surface damage (Fig. 5) in this case, and the fact that the Zn concentration was not monitored after chemomechanical polishing, it is possible that an inferior surface was present for LPE growth. The second explanation is that the addition of Zn to the vapor in the annealing process actually leads to fewer defects at all depths in the substrate. This would lead to improved epilayer quality as compared to the Cd-only anneal.

Hall samples were scribed from a corner (with good layer morphology) of each HgCdTe layer. The samples

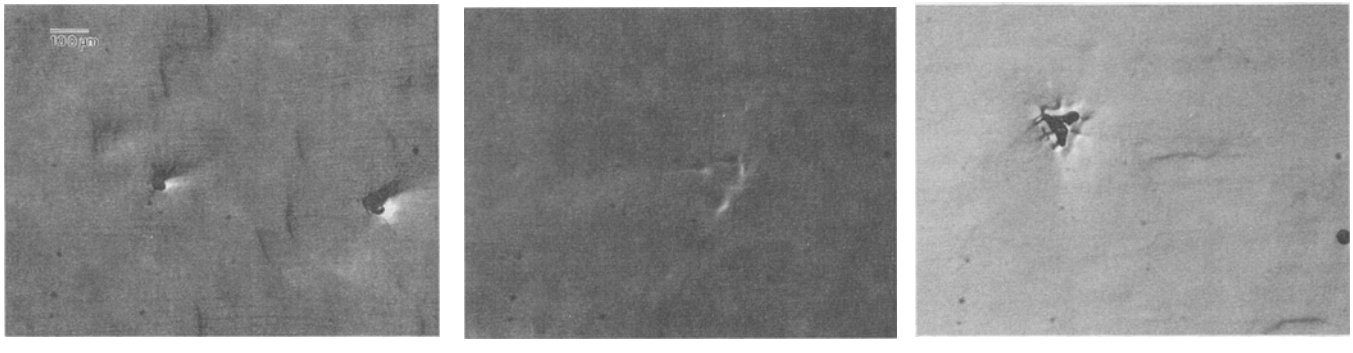

a b c

Fig. 8. Morphological defect features in the LPE HgCdTe layers grown on transparent and annealed (700°C for seven days in Cd vapor) substrates. Defects shown in (a), (b), and (c) do not correlate with inclusions in the substrate.

were then annealed with Hg overpressure at 250°C for 24 h to fill in the Hg vacancies that are always created during LPE growth. The Hall effect data measured at 77K show that, within the accuracy of the Hall test, the carrier concentration and mobility are the same for layers grown on substrates that had received the Cd-Zn anneal, as for layers grown on unannealed control samples. Similar results were obtained for layers on Cd annealed substrates.

The morphology of the substrate-layer interface was examined on cleaved cross sections of the LPE layer under the infrared polarizing microscope with reflected light. No difference was found between layers grown on annealed and unannealed substrates. However, unless the substrate has numerous defects and those defects happen to be exposed by the cleavage, it is very difficult to catch any features at the interface.

CONCLUSIONS

Detailed characterization of large (>10 μm) second phase inclusion defects in vertical-Bridgman-grown CdZnTe has revealed two categories that correlate with the IR transmission characteristics of the material. We have found star-shaped defects with a central core containing Cd in only the IR-transparent materials and call this type category 1. Category 2 type inclusions of triangular, hexagonal, and irregular shapes, which contained excess Te were found only in IR-absorbing materials. In addition, small voids which looked like precipitates (typically round) under the IR microscope were also observed, more often in the absorbing materials. An anneal in Cd vapor was able to correct the IR transmission in absorbing CdZnTe and decrease the sizes of both categories of defects. However, reduction in size or elimination of the second phase was more effective in case of category 2 Te inclusions than the category 1 Cd inclusions. Presumably, annealing in a Te atmosphere would be more effective for elimination of Cd inclusions but this was not attempted. It was also found that Cd vapor annealing leaves the CdZnTe surfaces defective due to a loss of Zn. The surface damage depth ranged from 50 to 175 μm and was significantly greater in case of absorbing substrates. Annealing in a vapor produced by a $Cd_{1-x}Zn_x$ (x = 0.005) alloy on the other hand, minimized the surface damage depth without any loss of Zn, and the annealing behavior on inclusions was similar to that with Cd vapor.

SIRIS spatial imaging of Cu concentrations in and around Cd and Te inclusions in the CdZnTe matrix showed ten times higher Cu concentration in the Te inclusion and 100 times higher Cu in the Cd inclusion, compared to that in the CdZnTe matrix. These initial data support the hypothesis that copper preferentially migrates to Te/Cd second phase regions. Further experiments need to be performed to determine whether Cu has a greater affinity for Cd than Te.

With regard to the epitaxial HgCdTe layer quality, correlation of pinhole-like morphological defects with underlying near-surface inclusions in the unannealed substrate was found. But layers on Cd-annealed substrates had other irregular shaped defects with no obvious correlation with underlying substrate defects. However, the density of these irregular shaped defects was much lower in layers grown on Cd-Zn annealed substrates. Crystal quality of the near-surface region of Cd-Zn annealed substrates was much improved due to prevention of Zn loss during annealing. Hall effect data measured at 77K on HgCdTe layers did not show significant differences in carrier concentration or mobility values between layers grown on annealed and unannealed substrates.

ACKNOWLEDGMENTS

Work supported by ARPA through the U.S. Air Force Materials Directorate, on Contract No. F33615-93-C-5367.

REFERENCES

1. D.R. Rhiger, J.M. Peterson and G.M. Venzor, unpublished (IRIS Materials Mtg., Aug. 1994).
2. S.M. Johnson, D.R. Rhiger, J.P. Rosbeck, J.M. Peterson, S.M. Taylor and M.E. Boyd, *J. Vac. Sci. Technol. B* 10, 1499 (1992).
3. D.R. Rhiger, R.D. Rodriguez and J.M. Peterson, unpublished (IRIS Detector Mtg., Aug. 1991).
4. J.H. Tregilgas, T.L. Polgreen and M.C. Chen, *J. Cryst. Growth* 86, 460 (1988).
5. S. Sen, S.M. Johnson, J.A. Kiele, W.H. Konkel and J.E. Stannard, *Mat. Res. Soc. Symp. Proc.* 161, 3 (1990).
6. H.R. Vydyanath, J. Ellsworth, J.J. Kennedy, B. Dean. C.J. Johnson, G.T. Neugebauer, J. Sepich and P. Liao, *J. Vac. Sci. Technol. B* 10, 1476 (1992).
7. H.R. Vydyanath, J.A. Ellsworth, J.B. Parkinson. J.J. Kennedy, B. Dean, C.J. Johnson, G.T. Neugebauer, J. Sepich and P. Liao, *J. Electron. Mater.* 22, 1073 (1993).
8. R. Korenstein, R. J. Olson, D. Lee, P.K. Liao and C.A. Castro, *J. Electron. Mater.* 24, 511 (1995).
9. J.P. Tower, S.P. Tobin, P.W. Norton, A.B. Bolong, A. Socha, J.H. Tregilgas, C.K. Ard and H.F. Arlinghaus, *J. Electron. Mater.* 25, 1183 (1996).
10. M.H. Kalisher, P.E. Herning and T. Tung, *Prog. Crystal Growth Charact.* 29, 41 (1994).
11. H.F. Arlinghaus, M.T. Spaar, N. Thonnard, A.W. McMahon, T. Tanigaki, H. Shichi and P.H. Holloway, *J. Vac. Sci. Technol. A* 11, 2317 (1993).
12. H.F. Arlinghaus, M.T. Spaar and N. Thonnard, *J. Vac. Sci. Technol. A* 8, 2318 (1990).
13. H.F. Arlinghaus, M.T. Spaar, N. Thonnard, A.W. McMahon and K.B. Jacobson, *Optical Methods for Ultrasensitive Detection and Analysis: Techniques and Applications*, ed. B.L.Fearey, SPIE Proc. 1435, 26 (1991).
14. S.M. Johnson, S. Sen, W.H. Konkel and M.H. Kalisher, *J. Vac. Sci. Technol. B* 9, 1897 (1991).
15. H.R. Vydyanath, J.A. Ellsworth, R.F. Fisher, J.J. Kennedy, C.J. Johnson and G.T. Neugebauer, *J. Electron. Mater.* 22, 1067 (1993).
16. S. Sen, J.E. Stannard, S.M. Johnson, H.F. Arlinghaus and G.I. Bekov, *J. Electron. Mater.* 24, 515 (1995).
17. K. Nakagawa, K. Maeda and S. Takeuchi, *Appl. Phys. Lett.* 34, 574 (1979).
18. J.G. Brion, C. Mewes, I. Hahn and U. Schäufele, *J. Cryst. Growth* 134, 281 (1993).
19. R.D.S. Yadava, R.K. Bagai and W.N. Borle, *J. Electron. Mater.* 21, 1001 (1992).
20. J. Shen, D.K. Aidun, L. Regel and W.R. Wilcox, *J. Cryst. Growth* 132, 250 (1993).